Supplementary Materials

X-ray structures of AMPA receptor–cone snail toxin complexes illuminate activation mechanism

Lei Chen, Katharina L. Duerr and Eric Gouaux

Materials and Methods

Supplementary Tables

Supplementary Figure Legends

Supplementary Movie Legends

Supplementary Figures

Supplementary Materials

Materials and Methods

Expression and purification of toxin

The cDNA of mature con-ikot-ikot toxin (amino acid 38-123 of UniportKB number P0CB20) was chemically synthesized and verified by double strand DNA synthesis. The DNA fragment was inserted into pET32b for large-scale expression. One Strep-tag and a HRV 3C cleavage site were introduced between the Trx fusion tag and con-ikot-ikot. The resulting vector was transformed into Origami B (DE3) *E. coli* cell for expression. Cultures were induced with 100 μM IPTG at 16 ^{o}C when the OD_{600} reached 0.8-1.0. Cells were harvested 16-20 h post-induction and broken by sonication in lysis buffer (50 mM Tris pH8.0, 150 mM NaCl, 5 mM EDTA, 1 mM PMSF. 0.8 μM aprotinin, 2 μg/ml leupeptin, 2 mM pepstatin A). The supernatant was recovered by ultracentrifugation at 40,000 rpm using a Ti45 rotor for 20 min and loaded onto an XK16 column packed with 10 ml Strep-Tactin superflow high capacity resin. The column was extensively washed by Strep-buffer A (20 mM Tris pH 8.0 150 mM NaCl, 1 mM EDTA) and step-eluted by Strep-buffer B (20 mM Tris pH 8.0 150 mM NaCl, 1mM EDTA 2.5 mM desthiobiotin). The eluted protein was concentrated using a 30 kDa cut-off spin concentrator to smaller volume and 3C protease (1:200) was added to cleave off the Trx tag (4°C overnight). After the digest, 2 volumes of methanol was added to the digest and the mixture was incubated in 37°C for 10 min to fully precipitate the cleaved Trx-tag and non-specifically cross-linked product. The supernatant was recovered by centrifugation at 4,000 rpm for 10 min and concentrated using 10 kDa spin concentrator. The buffer was also exchanged to 20 mM Tris, pH 8.0 150 mM NaCl, 1 mM EDTA during concentration. The concentrated supernatant was incubated at RT for 1.5 days before 1 mM GSH was added and the sample was further incubated at RT overnight to promote correct disulfide bond formation. The protein sample was diluted by 30 mM NaAc, pH 4.5 and loaded onto 1 ml SP-sepharose prepacked high performance column. The protein was eluted using a 100 mM-250 mM NaCl gradient. The fractions that contain functional toxin dimer were identified by SDS-PAGE gel and concentrated using a 10 kDa spin concentrator and loaded onto a Superdex 75 column equilibrated in 10 mM Tris pH 8.0, 150 mM NaCl.

The toxin dimer fractions were pooled and concentrated using a 10 kDa spin concentrator to 2 mg/ml and stored at 4°C for crystallization or functional studies. A typical yield of toxin is about 200 µg from 12 L culture.

Construct design and purification of the GluA2 AMPA receptor

Further modifications of the GluA2 AMPA receptor crystallization construct was based on the previous $GluA2_{cryst}$ construct used for the ZK-bound structure (*6*). By mass spectrum, a low occupancy non-canonical glycosylation site at N461 was identified in GluA2. The N461D mutation was therefore introduced to increase the chemical homogeneity. Next, the replacement of amino acid sequence 'RETQSS' on the M1-M2 loop by 'E' and a two amino acid deletion (LP) from the ATD-LBD linker of GluA2*flip* (GluA2*i*) (*31*) had beneficial effects on crystal diffraction quality. Finally, a combination of ten point mutations in the TM region (C528A, G535L, L577F, S580A, G582K, A583L, M585F, G598A, G602A, C815A) was essential to enhance the stability of activated complexes. The resulting construct with these ten mutations preserves gating function of the receptor yet resulted in smaller currents in whole cell recordings (Fig. S2B, S2D). This modified construct yielded a complete data set of the GluA2-toxin complex to 4.5 Å and the structure was solved by molecular replacement using individual domains. By close examination of the structure, we found that the long side chains of K188 (amino acid number in 3KG2) in ATD from chain A and chain D caused a clash with the toxin. Thus, we mutated K188 to a glycine to generate $GluA2_{cryst1}$ construct. The resulting $GluA2_{cryst1}$ construct can give complete data sets of the GluA2-toxin complex to beyond 4 Å resolution. To further analyze whether the thermostabilizing mutations and the N461D mutation affect GluA2-toxin structure, we generated the $GluA2_{cryst2}$ construct which has only C815A mutation on TMD and no N461D mutation, while having the same inter-domain linker as $GluA2_{cryst1.}$ GluA2 protein was expressed in HEK293 $GntI^-$ cells (*32*) via the BacMam system (*33*) and Endo H treated prior to crystallization.

Crystallization

For toxin crystallization in the $P3_121$ crystal form, purified toxin at 2 mg/ml was mixed with well buffer (0.1 M MES pH 5.4-6.0, 11%-20% ethanol, 0.2 M $ZnAc_2$) at 1:1 ratio. Crystals were grown at room

temperature by hanging drop method and transferred to cryo protectant (0.1M MES pH 6.0, 0.2 M $ZnAc_2$, 15% ethanol, 35% glycerol) and frozen in liquid nitrogen. For the toxin $P2_1$ crystal form, con-ikot-ikot at 3 mg/ml was mixed with well buffer (0.1 M Tris pH 8.5, 35% methanol, 16% PEG3350) at 1:1 ratio. Crystals were cryo-protected by transferring into 0.1 M Tris pH 8.5, 30% methanol, 16% PEG3350, 30% ethylene glycol and frozen in liquid nitrogen.

For the receptor-toxin complex, receptor protein (3 mg/ml, in 1 mM C_{11}thio-maltoside, 10 mM MES pH 6.3, 150 mM NaCl) was mixed with toxin at a molar ratio of 1:1.5 (receptor : toxin). (R,R)-2b and KA (or FW) (Fig. S6D, E, F) were added to final concentrations of 50 µM and 1 mM, respectively. Crystals were grown by hanging drop setup. The protein sample was mixed with well buffer (0.1 M MES pH 5.8-6.3, 0.1 M NaCl, 5%-6% PEG3350) at 1:1 ratio at 4^oC. Crystals appear in 1-3 days and grow to maximum size in 1 week. Crystals were harvested by a single step transfer into cryo-protectant (0.1 M MES pH 6.0, 6% PEG3350, 25% ethylene glycol, 1 mM C_{11}thio-maltoside, 1 mM FW or kainate, 50 µM (R,R)-2b) and frozen in liquid nitrogen.

Data collection and structure determination

Zn-based MAD data (*34*) of con-ikot-ikot $P3_121$ crystal form data sets were collected at SSRL12-2 at 1.281 Å (peak), 1.262 Å (remote) and 1.284 Å (edge). Sulfur anomalous signals were measured from the same crystal using x-ray of wavelength 1.75 Å. Datasets were processed using HKL2000 (*35*).Initial phases were obtained by phenix.autosol running in MAD mode (*36*). Two zinc sites were found and provided sufficient phasing power to generate an interpretable map. An initial model was build manually using COOT and register assignment were greatly aided by phased anomalous difference maps from sulfur. The final structure model was refined using PHENIX (*37*) and COOT (*38*) against the data set collected at 1.75 Å because it has the highest resolution and redundancy. The $P2_1$ crystal form data set was collected at ALS 5.0.2. The structure was solved by molecular replacement using the $P3_121$ crystal form structure and refined by PHENIX and COOT.

The receptor-toxin complex data sets were processed by XDS (*39*) and aimless in CCP4 (*40*). Structures were solved by molecular replacement using individual domains as search models with Phaser

in CCP4 and were further refined using Phenix and COOT. B-factor sharpening with -100Å^2 was used for side-chain rotamer assignment. Density of M2 is not sufficient for confident model building and M2 is omitted in all the receptor models.

Mercury-labeling of cysteine mutant S635C is achieved by soaking crystals with methyl mercury chloride for two days. Anomalous data was collected at 1Å. An initial model was generated by molecular replacement using $GluA2_{cryst1}$-toxin complex structure as search model and further refined using a rigid body protocol. Anomalous map was calculated using rigid body refined model as phase source.

Receptor toxin complex formation assay

Purified receptors are mixed with crude *Conus striatus* venom or purified recombinant con-ikot-ikot toxin with or without 1mM FW. The mixtures are separated on a Superose 6 column and receptor peak fractions were pooled, concentrated and separated by SDS-PAGE. Proteins were identified by silver staining.

^{3}H-FW binding

An SBP-tag was introduced after the GFP His_8 tag of the crystallization construct to generate the expression vector for scintillation proximity assay (SPA) experiments (*41*). SBP-tagged protein was expressed in HEK293 GntI$^-$ cells and purified by IMAC. Receptor concentration was estimated by UV_{280}. All SBP binding experiments were carried out in FSEC buffer (20 mM Tris pH 7.5, 150 mM NaCl, 0.5 mM $C_{12}M$). The binding conditions were optimized to 50 nM receptor subunit and 0.5 mg/ml PVT-streptavidin beads. Hot FW and cold FW were mixed in 1:10 ratio and 0.5 mM quisqualate was used to estimate non-specific binding. Total counts were determined in triplicate and background readings were determined as duplicates with 2 minutes reading time per well. Results shown in this work were obtained from readings after 24 hours at room temperature. Modulator (R,R)-2b was added at 20 μM, Con-ikot-ikot was added at 1 μM final concentration.

Electrophysiology

Whole-cell recordings were carried out with HEK293 GntI$^-$ cells 24–48□h after transfection with plasmid DNA encoding the C-terminal GFP fused rat GluA2*i* receptor constructs. Pipettes were pulled

and polished to 2–5 MΩ resistance and filled with internal solution containing (in mM): 75 CsCl, 75 CsF, 5 EGTA, 10 HEPES pH 7.3. External solution contained (in mM): 160 NaCl, 2.4 KCl, 4 $CaCl_2$, 4 $MgCl_2$, 10 mM HEPES pH 7.3. 10 mM L-glutamate was used to elicit the current. Continuous application of 300 µM CTZ was used to block desensitization. Toxin potentiation was measured by incubating 0.5 µM recombinant toxin with the clamped cell for 5 min. Non-tagged wild type rat TARPγ2 plasmid DNA was co-transfected with I633A GluA2 plasmid DNA for co-expression.

FACS

GntI$^-$ cells in suspension were transfected by plasmid DNA encoding the C-terminal GFP fused rat GluA2i receptor constructs. Cells were harvested 48 hours post-transfection and washed with PBS without Ca^{2+}. Washed cells were incubated with primary antibody 15F1, a high affinity GluA2-specific mouse monoclonal antibody recognizing an epitope in ATD. Excessive primary antibody was washed off prior to incubating the cells with APC-labeled goat anti-mouse secondary antibody. After washing off excessive secondary antibody, the cells were loaded onto a Calibur instrument for FACS analysis.

Table S1 Crystallographic data collection and refinement statistics of GluA2-toxin complex structures

	FW + (R,R)-2b+toxin (4U5C)	**KA + (R,R)-2b+toxin (4U5D)**	**T625G KA + (R,R)-2b+toxin (4U5E)**	**A622T KA + (R,R)-2b+toxin (4U5B)**	**KA + (R,R)-2b+toxin (4U5F)**	**S635C KA + (R,R)-2b+toxin**
Construct	$GluA2_{cryst1}$	$GluA2_{cryst1}$	$GluA2_{cryst1}$T625G	$GluA2_{cryst1}$A622T	$GluA2_{cryst2}$	$GluA2_{cryst1}$S635C
Data collection	ALS 5.0.2	ALS 5.0.2	ALS 5.0.2	ALS 5.0.2	ALS 5.0.2	ALS 5.0.2
Space group	$P2_12_12$	$P2_12_12$	$P2_12_12$	$P2_12_12$	$P2_12_12$	$P2_12_12$
Cell dimensions a, b, c (Å)	163.07, 364.78, 109.75	161.51, 367.58, 109.38	161.27, 366.69, 109.01	161.52, 368.66, 109.15	160.29, 365.42, 108.86	161.23, 367.45, 107.73
Cell angles α, β, γ (°)	90.00, 90.00, 90.00	90.00, 90.00, 90.00	90.00, 90.00, 90.00	90.00, 90.00, 90.00	90.00, 90.00, 90.00	90.00, 90.00, 90.00
Resolution (Å)*	148.87-3.69 (3.78-3.69)	97.62-3.52 (4.29-4.14)	97.41-3.50 (4.12-3.98)	90.44-3.50 (3.85-3.74)	146.79-3.51 (4.28-4.13)	147.64-7.89 (8.00-7.89)
Completeness	98.2(95.1)	96(97.3)	98.8(98.3)	96.1(96.7)	98.4(99.0)	99.7(100.0)
Multiplicity	3.7(3.6)	3.2(3.2)	3.7(3.8)	4.1(4.1)	3.7(3.7)	7.8(8.2)
I/σI	11.8(1.9)	5.1(2.0)	9.4(1.5)	7.5(1.6)	8.3(2.1)	17.2(2.7)
R_{merge} (%)	7.8(66.6)	12.0(49.6)	15.1(99.2)	14.4(105.6)	13.6(71.4)	8.7(81.6)
Anisotropy (Å: a*/b*/c*)†	3.7,3.7,3.7	3.9,4.1,3.5	3.9,3.9,3.5	3.7,4.0,3.5	3.9,3.7,3.7	
Refinement						
Resolution (Å)	19.98-3.69	19.99-3.58	19.99-3.51	20.00-3.50	19.99-3.70	
No. of reflections	69576	60144	64765	65227	64195	
R_{work}/R_{free} (%)‡	21.34/25.89	24.74/29.31	23.45/28.02	21.84/25.94	24.96/29.50	
No. of atoms total	24451	23715	23731	23749	23695	
Ligand	180	180	180	180	180	
Average *B*-factor (A^2)	138.4	149.5	160.4	159.4	151.5	
Protein	138.5	149.7	160.5	159.5	151.6	
Ligand	116.2	134.7	141.0	144.1	133.8	
R.m.s. deviations						
Bond lengths (Å)	0.005	0.003	0.006	0.004	0.004	
Bond angles (°)	0.981	0.762	0.873	0.814	0.803	
Ramachandran plot						
Favored (%)	96.2	97.1	97.5	97.4	97.1	
Allowed (%)	3.8	2.8	2.5	2.6	2.9	
Disallowed (%)	0.00	0.03	0.00	0.00	0.00	

* The number in parenthesis is the shell at conventional cut off using I/σI=2 as criteria.

† Anisotropy truncation was performed using the anisotropy server (http://services.mbi.ucla.edu/anisoscale/).

‡ 5% of reflections were used for calculation of $R_{free.}$

Table S2 Crystallographic data collection and refinement statistics of toxin structures

	Crystal form1 (4U5G)				Crystal form2 (4U5H)
Data collection	SSRL12-2				ALS 5.0.2
Wavelength(Å)	1.281(Zn Peak)	1.262(Zn Remote)	2.284(Zn Edge)	1.75(Sulfur)	1.00
Space group	*P* 3_121				*P*2_1
Cell dimensions a, b, c (Å)	56.499, 56.499, 86.782				42.910, 144.860, 48.600
Cell angles α, β, γ (°)	90.00, 90.00, 120.00				90.00, 94.63, 90.00
Resolution (Å)*	50.00-2.30 (2.34-2.3)	50.00-2.30 (2.34-2.3)	50.00-2.30 (2.34-2.3)	50.00-2.20 (2.24-2.2)	42.77-1.58 (1.62-1.58)
Completeness	99.7 (100.0)	99.7 (99.7)	99.7 (100.0)	99.8 (100)	99.3 (99.5)
Multiplicity	18.2 (17.4)	18.2 (15.8)	18.2 (17.7)	35.0 (31.3)	3.7 (3.7)
I/σI	20.5 (3.5)	20.2 (3.0)	20.2 (3.2)	30.8 (4.7)	9.3 (2.4)
R_{merge} (%)	11.8 (59.4)	11.8 (65.7)	11.1 (61.2)	11.5 (55.1)	9.2 (59.0)
Refinement					
Resolution (Å)				19.83-2.20	19.90-1.58
No. of reflections				8517	79955
R_{work}/R_{free} (%)†				20.20/23.85	19.37/21.12
No. of atoms				1287	5799
Protein				1260	5169
Ion				2	-
Water				25	630
Average B-factor (Å^2)				44.6	15.71
Protein				44.6	14.61
Ion				34.3	-
Water				43.72	24.8
R.m.s. deviations					
Bond lengths (Å)				0.009	0.005
Bond angles (°)				1.325	1.066
Ramachandran plot					
Favored (%)				98.8	98.8
Allowed (%)				1.2	1.2
Disallowed (%)				0	0

* The number in parenthesis is the shell at conventional cut off using I/σI=2 as criteria.

† 5% of reflections were used for calculation of $R_{free.}$

Supplementary Figure Legends

Fig. S1. Biochemical properties and disulfide bond linkage of con-ikot-ikot toxin. (**A**) Non-reducing SDS-PAGE gel of purified recombinant toxin. (**B**) Elution profile of purified recombinant toxin on a Superdex 75 size exclusion chromatography column is shown in red. The elution peaks of standards with molecular masses of 29.0 kDa and 12.4kDa are shown in grey. The molecular weight of recombinant toxin monomer is 9.7 kDa. (**C**) Disulfide linkage of a pattern of con-ikot-ikot toxin. The helices of toxin are shown in magenta. Cysteine positions are labeled as "C" in yellow. The linkages between cysteine resides, as determined by the crystal structure, are indicated by yellow lines. There are 10 intermolecular disulfide bonds and 3 intra-molecular bonds for a total of 13 disulfide bonds.

Fig. S2. Action of con-ikot-ikot toxin on GluA2 receptors. (**A,B,C,D,E**) Whole cell patch clamp recording of the GluA2 receptor. Black bars above the trace show application of 10mM glutamate. Black arrows show incubation of the clamped cell with toxin for 5-10 min. Recordings on wild type GluA2 are shown in panels A and C. Recordings on $GluA2_{cryst1}$ are shown in panels B and D. Recordings on $GluA2_{cryst2}$ are shown in panels E. Arrows in panel A and B denote incubation of crude *Conus Striatus* venom. Arrows in panel C,D and E denote incubation with 500 nM of recombinant venom. (**F**) Scintillation proximity assay (SPA) binding experiments measuring the ^{3}H FW binding to the $GluA2_{cryst1}$ construct in the presence of (R,R)-2b, toxin, and (R,R)-2b and toxin. Data are fitted by single site binding model. Shown are the mean values ± standard error of the mean based on in three replicates. Because we obtain crystals in the same crystal form without modulator and because toxin alone potently blocks desensitization, we propose that the toxin alone stabilizes the D1 – D1 interface in an intact conformation as in toxin-modulator complex observed here, as they share the same mechanism to prevent desensitization but bind to the receptor at different sites.

Fig. S3. GluA2-toxin interactions and LBD clamshell closure. (**A**) Sequence alignment of selected iGluRs amino acid sequences at the key sites for toxin interaction. Conserved residues are shown in red.

(**B**) Structure comparison of the KA+toxin+(R,R)-2b structure (shown in gray) and the FW+toxin+(R,R)-2b structure (LBD shown in blue and toxin shown in purple). Only the E subunit of the toxin and the LBD from the A subunit of GluA2 are shown. The toxin E subunit is used in structural alignment. The Cα atoms of K458 are used as marker atoms and are shown as spheres. The Cα of K458 of the apo sLBD following super imposition of the D2 lobe is shown as orange sphere. (**C**) Close-up view of the GluA2-toxin interaction sites. Key interactions between toxin E48 and GluA2 R660 and between toxin Q37 and GluA2 R453 are shown. Notably, there are 3.2 Å and 7.0 Å shifts of the Cα atoms of K458 between KA and FW and between KA and apo structures, respectively, due to different degrees of clamshell closure. (**D**) Reducing SDS-PAGE analysis of the SEC peak of the GluA2-toxin complex. Sample (a) is full length GluA2 protein mixed with crude *Conus striatus* venom, in the presence of FW. Sample (b) is GluA2 protein mixed with purified recombinant toxin, in the presence of FW. Sample (c) is the same as Sample (b) except without FW. Reduced toxin monomer position is labeled by an asterisk. (**E).** The soluble LBD structure with KA bound (PDB code 1FW0), showing the two distances ξ1 and ξ2 used to describe domain closure. ξ1 is the distance between the centers of mass (COMs) of residues 479–481 and residues 654–655. ξ_2 is the distance between the COMs of residues 401–403 and residues 686–687. Distances are plotted in panel (**F**).

Fig. S4. **I633 coupling switch mutants**. (**A,D,G,J,M**) Whole cell patch clamp recordings of wild type GluA2 (A), the I633A mutant (D), the I633E mutant (G) and the I633A mutant coexpressed with TARP γ2 (M). The black bar above the traces denotes application of 10 mM glutamate. The gray bar above the traces denotes continuous application of 300 μM cyclothiazide (CTZ). Statics of steady state currents recorded from wild type GluA2, I633A and I633E mutants are shown in (J) data is presented as ±SEM, n=5. (**B,E,H**) Fluorescence-detection size-exclusion chromatography (FSEC) profiles of wild-type GluA2 (B), the I633A mutant (E) and the I633E mutant (H). (**C,F,I,K,L**) FACS analysis of cell surface expression of wild-type GluA2 (C), I633A (F) and I633E (I). Negative control of untransfected cell with both primary and secondary antibodies is shown in panel K. A negative control experiment using cells

transfected with GFP-tagged wild-type GluA2 and secondary antibodies is shown in L. (**N**) Sequence alignment of selected iGluR sequences near the I633 coupling switch site. Residue I633 or its equivalent is in red.

Fig. S5. Electron density maps. (**A**) A 2mFo-DFc electron density map of the toxin in $GluA2_{cryst1}$, FW+(R,R)-2b+toxin structure. The map is contoured at 1.5σ. (**B-F**) A 2mFo-DFc map of the D2-M3 linker and M3 of chain B and D. Electron density map of the $GluA2_{cryst1}$, FW+(R,R)-2b+toxin structure is shown in panel B and the map is contoured at 0.9σ. An electron density map of the $GluA2_{cryst1}$, KA+(R,R)-2b+toxin structure is shown in panel C and the map is contoured at 0.9σ. An electron density map of $GluA2_{cryst2}$, KA+(R,R)-2b+toxin is shown in panel D and the map is contoured at 0.9σ. An electron density map of GluA2.A622T, KA+(R,R)-2b+toxin is shown in panel E and the map is contoured at 0.8σ. An electron density map of GluA2.T625G, KA+(R,R)-2b+toxin is shown in panel F and the map is contoured at 0.8σ. (**G**) A phased anomalous difference electron density map of Hg-labeled S635C at LBD-TM linker region. The map is contoured at 3.0σ.

Fig. S6. Stereo figures of structure comparison between GluA2 KA+toxin+(R,R)-2b and A622T GluA2 mutant KA+toxin+(R,R)-2b complex. The main chain atoms of the site of mutation, A622, are illustrated in orange. (**A**) Cα trace of the LBD D2 to M3 connections in the B/D subunits. The structure of the GluA2 KA+toxin+(R,R)-2b elements are shown in gray and those derived from the A622T GluA2 mutant KA+toxin+(R,R)-2b complex are shown in green. (**B**) The LBD D2 to M3 connections in A/C subunits. The structure of the GluA2 KA+toxin+(R,R)-2b complex is shown in gray and the structure of the A622T GluA2 KA+toxin+(R,R)-2b complex is shown in blue. (**C**) The close-up view of M3 tip and I633 binding site of B/D subunit. The structure of the GluA2 KA+toxin+(R,R)-2b elements (I633-uncoupled structure) are shown in gray and those derived from the A622T GluA2 mutant KA+toxin+(R,R)-2b complex (I633-coupled structure) are shown in green. Distances between Cα of V626 from intact M3 tip and Cαs of S631 from both structures are shown by dash lines. Chemical structure of positive modulator (R,R)-2b (**D**), FW (**E**) and KA (**F**).

Supplementary Movie Legends

Suppl. Movie M1: Morph illustrating the transition from an antagonist-bound GluA2 receptor conformation to a toxin + partial agonist FW + modulator (R,R)-2b-bound GluA2 conformation. This movie illustrates the symmetrical binding of the toxin dimer (magenta cartoon representation) between ATD and LBD layers of the GluA2 receptor, involving both intra- and inter-dimer interactions with the D1 lobes of all four chains, and with D1 and D2 lobes of the AC pair. Apart from toxin binding, the movie also highlights some key structural changes in the LBD region upon activation of the receptor by the partial agonist FW, including domain closure and the concomitant separation of the D2 lobes. The movie cycles several times between the previously published structure in complex with antagonist ZK200775 (ZK) and a toxin/receptor complex structure with partial agonist FW and the positive allosteric modulator (R,R)-2b. The respective current state in the movie (ZK or FW+(R,R)-2b)+toxin) is indicated by the label in the left lower corner. Ligand and modulator (R,R)-2b molecules are shown as grey or orange spheres, respectively. Receptor chains are colored the same as in previous figures (chains A and C in blue, chains B and D in green). The ATD layer of the receptor is only shown once for the ZK-bound structure at the beginning of the movie and omitted in the rest of the movie.

Suppl. Movie M2: Morph illustrating the transition from an antagonist-bound GluA2 receptor conformation to a toxin + partial agonist KA + modulator (R,R)-2b-bound GluA2 conformation. The movie shows the same transition and receptor views as Movie M1 except here the toxin binds to the receptor in presence of the partial agonist KA and modulator (R,R)-2b.

Supplementary Materials

Activation mechanism of AMPA receptors illuminated by complexes with cone snail toxin allosteric potentiator and orthosteric agonists

Lei Chen, Katharina L. Duerr and Eric Gouaux

Materials and Methods

Supplementary Tables

Supplementary Figure Legends

Supplementary Movie Legends

Supplementary Figures

Supplementary Materials

Materials and Methods

Expression and purification of toxin

The cDNA of mature con-ikot-ikot toxin (amino acid 38-123 of UniportKB number P0CB20) was chemically synthesized and verified by double strand DNA synthesis. The DNA fragment was inserted into pET32b for large-scale expression. One Strep-tag and a HRV 3C cleavage site were introduced between the Trx fusion tag and con-ikot-ikot. The resulting vector was transformed into Origami B (DE3) *E. coli* cell for expression. Cultures were induced with 100 μM IPTG at 16 ^{o}C when the OD_{600} reached 0.8-1.0. Cells were harvested 16-20 h post-induction and broken by sonication in lysis buffer (50 mM Tris pH8.0, 150 mM NaCl, 5 mM EDTA, 1 mM PMSF. 0.8 μM aprotinin, 2 μg/ml leupeptin, 2 mM pepstatin A). The supernatant was recovered by ultracentrifugation at 40,000 rpm using a Ti45 rotor for 20 min and loaded onto an XK16 column packed with 10 ml Strep-Tactin superflow high capacity resin. The column was extensively washed by Strep-buffer A (20 mM Tris pH 8.0 150 mM NaCl, 1 mM EDTA) and step-eluted by Strep-buffer B (20 mM Tris pH 8.0 150 mM NaCl, 1mM EDTA 2.5 mM desthiobiotin). The eluted protein was concentrated using a 30 kDa cut-off spin concentrator to smaller volume and 3C protease (1:200) was added to cleave off the Trx tag (4°C overnight). After the digest, 2 volumes of methanol was added to the digest and the mixture was incubated in 37°C for 10 min to fully precipitate the cleaved Trx-tag and non-specifically cross-linked product. The supernatant was recovered by centrifugation at 4,000 rpm for 10 min and concentrated using 10 kDa spin concentrator. The buffer was also exchanged to 20 mM Tris, pH 8.0 150 mM NaCl, 1 mM EDTA during concentration. The concentrated supernatant was incubated at RT for 1.5 days before 1 mM GSH was added and the sample was further incubated at RT overnight to promote correct disulfide bond formation. The protein sample was diluted by 30 mM NaAc, pH 4.5 and loaded onto 1 ml SP-sepharose prepacked high performance column. The protein was eluted using a 100 mM-250 mM NaCl gradient. The fractions that contain functional toxin dimer were identified by SDS-PAGE gel and concentrated using a 10 kDa spin concentrator and loaded onto a Superdex 75 column equilibrated in 10 mM Tris pH 8.0, 150 mM NaCl.

The toxin dimer fractions were pooled and concentrated using a 10 kDa spin concentrator to 2 mg/ml and stored at 4°C for crystallization or functional studies. A typical yield of toxin is about 200 µg from 12 L culture.

Construct design and purification of the GluA2 AMPA receptor

Further modifications of the GluA2 AMPA receptor crystallization construct was based on the previous $GluA2_{cryst}$ construct used for the ZK-bound structure (*1*). By mass spectrum, a low occupancy non-canonical glycosylation site at N461 was identified in GluA2. The N461D mutation was therefore introduced to increase the chemical homogeneity. Next, the replacement of amino acid sequence 'RETQSS' on the M1-M2 loop by 'E' and a two amino acid deletion (LP) from the ATD-LBD linker of GluA2*flip* (GluA2*i*) had beneficial effects on crystal diffraction quality. Finally, a combination of ten point mutations in the TM region (C528A, G535L, L577F, S580A, G582K, A583L, M585F, G598A, G602A, C815A) was essential to enhance the stability of activated complexes. The resulting construct with these ten mutations preserves gating function of the receptor yet resulted in smaller currents in whole cell recordings (Fig. S2B, S2D). This modified construct yielded a complete data set of the GluA2-toxin complex to 4.5 Å and the structure was solved by molecular replacement using individual domains. By close examination of the structure, we found that the long side chains of K188 (amino acid number in 3KG2) in ATD from chain A and chain D caused a clash with the toxin. Thus, we mutated K188 to a glycine to generate $GluA2_{cryst1}$ construct. The resulting $GluA2_{cryst1}$ construct can give complete data sets of the GluA2-toxin complex to beyond 4 Å resolution. To further analyze whether the thermostabilizing mutations and the N461D mutation affect GluA2-toxin structure, we generated the $GluA2_{cryst2}$ construct which has only C815A mutation on TMD and no N461D mutation, while having the same inter-domain linker as $GluA2_{cryst1.}$ GluA2 protein was expressed in HEK293 $GNTI^-$ cells via the BacMaM system and endo H treated prior to crystallization.

Crystallization

For toxin crystallization in the $P3_12_1$ crystal form, purified toxin at 2 mg/ml was mixed with well buffer (0.1 M MES pH 5.4-6.0, 11%-20% ethanol, 0.2 M $ZnAc_2$) at 1:1 ratio. Crystals were grown at room

temperature by hanging drop method and transferred to cryo protectant (0.1M MES pH 6.0, 0.2 M $ZnAc_2$, 15% ethanol, 35% glycerol) and frozen in liquid nitrogen. For the toxin $P2_1$ crystal form, con-ikot-ikot at 3 mg/ml was mixed with well buffer (0.1 M Tris pH 8.5, 35% methanol, 16% PEG3350) at 1:1 ratio. Crystals were cryo-protected by transferring into 0.1 M Tris pH 8.5, 30% methanol, 16% PEG3350, 30% ethylene glycol and frozen in liquid nitrogen.

For the receptor-toxin complex, receptor protein (3 mg/ml, in 1 mM C_{11}thio-maltoside, 10 mM MES pH 6.3, 150 mM NaCl) was mixed with toxin at a molar ratio of 1:1.5 (receptor : toxin). (R,R)-2b and KA (or FW) (Fig. S6D, E, F) were added to final concentrations of 50 µM and 1 mM, respectively. Crystals were grown by hanging drop setup. The protein sample was mixed with well buffer (0.1 M MES pH 5.8-6.3, 0.1 M NaCl, 5%-6% PEG3350) at 1:1 ratio at 4^oC. Crystals appear in 1-3 days and grow to maximum size in 1 week. Crystals were harvested by a single step transfer into cryo-protectant (0.1 M MES pH 6.0, 6% PEG3350, 25% ethylene glycol, 1 mM C_{11}thio-maltoside, 1 mM FW or Kainate, 50 µM (R,R)-2b) and frozen in liquid nitrogen.

Data collection and structure determination

Zn-based MAD data of con-ikot-ikot $P3_121$ crystal form data sets were collected at SSRL12-2 at 1.281 Å (peak), 1.262 Å (remote) and 1.284 Å (edge). Sulfur anomalous signals were measured from the same crystal using x-ray of wavelength 1.75 Å. Datasets were processed using HKL2000(*2*).Initial phases were obtained by phenix.autosol running in MAD mode (*3*). Two zinc sites were found and provided sufficient phasing power to generate an interpretable map. An initial model was build manually using COOT and register assignment were greatly aided by phased anomalous difference maps from sulfur. The final structure model was refined using Phenix (*4*) and COOT (*5*) against the data set collected at 1.75 Å because it has the highest resolution and redundancy. The $P2_1$ crystal form data set was collected at ALS 5.0.2. The structure was solved by molecular replacement using the $P3_121$ crystal form structure and refined by Phenix (*4*) and COOT (*5*).

The receptor-toxin complex data sets were processed by XDS (*6*) and aimless in CCP4 (*7*). Structures were solved by molecular replacement using individual domains as search models with Phaser in CCP4

(*7*) and were further refined using Phenix(*4*) and COOT(*5*). B-factor sharpening with -100Å^2 was used for side-chain rotamer assignment. Density of M2 is not sufficient for confident model building and M2 is omitted in all the receptor models.

Hg-labeling of cysteine mutant S635C is achieved by soaking crystals with methyl mercury chloride for two days. Anomalous data was collected at 1Å. An initial model was generated by molecular replacement using GluA2$_{cryst1}$-toxin complex structure as search model and further refined using a rigid body protocol. Anomalous map was calculated using rigid body refined model as phase source.

Receptor toxin complex formation assay

Purified receptors are mixed with crude *Conus striatus* venom or purified recombinant con-ikot-ikot toxin with or without 1mM FW. The mixtures are separated on suprose 6 and receptor peak fractions were pooled, concentrated and seperated on SDS-PAGE. Protein were stained by silver staining.

^{3}H-FW binding

An SBP-tag was introduced after the GFP His$_8$ tag of the crystallization construct to generate the expression vector for scintillation proximity assay (SPA) experiments. SBP-tagged protein was expressed in HEK293 GNTI$^-$ cells and purified by IMAC. Receptor concentration was estimated by UV$_{280}$. All SBP binding experiments were carried out in FSEC buffer (20 mM Tris pH 7.5, 150 mM NaCl, 0.5 mM C_{12}M). The binding conditions were optimized to 50 nM receptor subunit and 0.5 mg/ml PVT-streptavidin beads. Hot FW and cold FW were mixed in 1:10 ratio and 0.5 mM quisqualate was used to estimate non-specific binding. Total counts were determined in triplicate and background readings were determined as duplicates with 2 minutes reading time per well. Results shown in this work were obtained from readings after 24 hours at room temperature. Modulator (R,R)-2b was added at 20 µM, Con-ikot-ikot was added at 1 µM final concentration.

Electrophysiology

Whole-cell recordings were carried out with HEK293 GNTI$^-$ cells 24–48h after transfection with plasmid DNA encoding the C-terminal GFP fused rat GluA2*i* receptor constructs. Pipettes were pulled and polished to 2–3 MΩ resistance and filled with internal solution containing (in mM): 75 CsCl, 75 CsF, 5

EGTA, 10 HEPES pH 7.3. External solution contained (in mM): 160 NaCl, 2.4 KCl, 4 $CaCl_2$, 4 MgCl2, 10 mM HEPES pH 7.3. 10 mM L-glutamate was used to elicit the current. Continuous application of 300 μM CTZ was used to block desensitization. Toxin potentiation was measured by incubating 0.5 μM recombinant toxin with the clamped cell for 5 min. Non-tagged wild type rat TARPγ2 plasmid DNA was co-transfected with I633A GluA2 plasmid DNA for co-expression.

FACS

Ric15 cells in suspension were transfected by plasmid DNA encoding the C-terminal GFP fused rat GluA2i receptor constructs. Cells were harvested 48 hours post-transfection and washed with PBS without Ca^{2+}. Washed cells were incubated with primary antibody 15F1, a high affinity GluA2-specific mouse monoclonal antibody recognizing an epitope in ATD. Excessive primary antibody was washed off prior to incubating the cells with APC-labeled goat anti-mouse secondary antibody. After washing off excessive secondary antibody, the cells were loaded onto Calibur for FACS analysis.

References

1. A. I. Sobolevsky, M. P. Rosconi, E. Gouaux, X-ray structure, symmetry and mechanism of an AMPA-subtype glutamate receptor. *Nature* **462**, 745 (Dec 10, 2009).
2. Z. Otwinowski, W. Minor, Processing of X-ray diffraction data collected in oscillation mode. *Meth. Enzymol.* **276**, 307 (1997).
3. P. H. Zwart *et al.*, Automated structure solution with the PHENIX suite. *Methods Mol Biol* **426**, 419 (2008).
4. P. D. Adams *et al.*, The Phenix software for automated determination of macromolecular structures. *Methods* **55**, 94 (Sep, 2011).
5. P. Emsley, K. Cowtan, Coot: model-building tools for molecular graphics. *Acta Crystallogr D Biol Crystallogr* **60**, 2126 (Dec, 2004).
6. W. Kabsch, Xds. *Acta Crystallogr D Biol Crystallogr* **66**, 125 (Feb, 2010).
7. N. CCP4 Project, The CCP4 suite: programs for protein crystallography. *Acta Crystallogr D Biol Crystallogr* **50**, 760 (Sep 1, 1994).

Table S1 Crystallographic data collection and refinement statistics of GluA2-toxin complex structures

	FW + (R,R)-2b+toxin (4U5C)	**KA + (R,R)-2b+toxin (4U5D)**	**T625G KA + (R,R)-2b+toxin (4U5E)**	**A622T KA + (R,R)-2b+toxin (4U5B)**	**KA + (R,R)-2b+toxin (4U5F)**	**S635C KA + (R,R)-2b+toxin**
Construct	$GluA2_{cryst1}$	$GluA2_{cryst1}$	$GluA2_{cryst1}$T625G	$GluA2_{cryst1}$A622T	$GluA2_{cryst2}$	$GluA2_{cryst1}$S635C
Data collection	ALS 5.0.2	ALS 5.0.2	ALS 5.0.2	ALS 5.0.2	ALS 5.0.2	ALS 5.0.2
Space group	$P2_12_12$	$P2_12_12$	$P2_12_12$	$P2_12_12$	$P2_12_12$	$P2_12_12$
Cell dimensions a, b, c (Å)	163.07, 364.78, 109.75	161.51, 367.58, 109.38	161.27, 366.69, 109.01	161.52, 368.66, 109.15	160.29, 365.42, 108.86	161.23, 367.45, 107.73
Cell angles α, β, γ (°)	90.00, 90.00, 90.00	90.00, 90.00, 90.00	90.00, 90.00, 90.00	90.00, 90.00, 90.00	90.00, 90.00, 90.00	90.00, 90.00, 90.00
Resolution (Å)*	148.87-3.69 (3.78-3.69)	97.62-3.52 (4.29-4.14)	97.41-3.50 (4.12-3.98)	90.44-3.50 (3.85-3.74)	146.79-3.51 (4.28-4.13)	147.64-7.89 (8.00-7.89)
Completeness	98.2(95.1)	96(97.3)	98.8(98.3)	96.1(96.7)	98.4(99.0)	99.7(100.0)
Multiplicity	3.7(3.6)	3.2(3.2)	3.7(3.8)	4.1(4.1)	3.7(3.7)	7.8(8.2)
I/σI	11.8(1.9)	5.1(2.0)	9.4(1.5)	7.5(1.6)	8.3(2.1)	17.2(2.7)
R_{merge} (%)	7.8(66.6)	12.0(49.6)	15.1(99.2)	14.4(105.6)	13.6(71.4)	8.7(81.6)
Anisotropy (Å: a*/b*/c*)†	3.7,3.7,3.7	3.9,4.1,3.5	3.9,3.9,3.5	3.7,4.0,3.5	3.9,3.7,3.7	
Refinement						
Resolution (Å)	19.98-3.69	19.99-3.58	19.99-3.51	20.00-3.50	19.99-3.70	
No. of reflections	69576	60144	64765	65227	64195	
R_{work}/R_{free} (%)‡	21.34/25.89	24.74/29.31	23.45/28.02	21.84/25.94	24.96/29.50	
No. of atoms total	24451	23715	23731	23749	23695	
Ligand	180	180	180	180	180	
Average *B*-factor (A^2)	138.4	149.5	160.4	159.4	151.5	
Protein	138.5	149.7	160.5	159.5	151.6	
Ligand	116.2	134.7	141.0	144.1	133.8	
R.m.s. deviations						
Bond lengths (Å)	0.005	0.003	0.006	0.004	0.004	
Bond angles (°)	0.981	0.762	0.873	0.814	0.803	
Ramachandran plot						
Favored (%)	96.2	97.1	97.5	97.4	97.1	
Allowed (%)	3.8	2.8	2.5	2.6	2.9	
Disallowed (%)	0.00	0.03	0.00	0.00	0.00	

* The number in parenthesis is the shell at conventional cut off using I/σI=2 as criteria.

† Anisotropy truncation was performed using the anisotropy server (http://services.mbi.ucla.edu/anisoscale/).

‡ 5% of reflections were used for calculation of $R_{free.}$

Table S2 Crystallographic data collection and refinement statistics of toxin structures

	Crystal form1 (4U5G)				Crystal form2 (4U5H)
Data collection	SSRL12-2				ALS 5.0.2
Wavelength(Å)	1.281(Zn Peak)	1.262(Zn Remote)	2.284(Zn Edge)	1.75(Sulfur)	1.00
Space group	*P* 3_121				*P*2_1
Cell dimensions a, b, c (Å)	56.499, 56.499, 86.782				42.910, 144.860, 48.600
Cell angles α, β, γ (°)	90.00, 90.00, 120.00				90.00, 94.63, 90.00
Resolution (Å)*	50.00-2.30 (2.34-2.3)	50.00-2.30 (2.34-2.3)	50.00-2.30 (2.34-2.3)	50.00-2.20 (2.24-2.2)	42.77-1.58 (1.62-1.58)
Completeness	99.7 (100.0)	99.7 (99.7)	99.7 (100.0)	99.8 (100)	99.3 (99.5)
Multiplicity	18.2 (17.4)	18.2 (15.8)	18.2 (17.7)	35.0 (31.3)	3.7 (3.7)
I/σI	20.5 (3.5)	20.2 (3.0)	20.2 (3.2)	30.8 (4.7)	9.3 (2.4)
R_{merge} (%)	11.8 (59.4)	11.8 (65.7)	11.1 (61.2)	11.5 (55.1)	9.2 (59.0)
Refinement					
Resolution (Å)				19.83-2.20	19.90-1.58
No. of reflections				8517	79955
R_{work}/R_{free} (%)†				20.20/23.85	19.37/21.12
No. of atoms				1287	5799
Protein				1260	5169
Ion				2	-
Water				25	630
Average B-factor (Å^2)				44.6	15.71
Protein				44.6	14.61
Ion				34.3	-
Water				43.72	24.8
R.m.s. deviations					
Bond lengths (Å)				0.009	0.005
Bond angles (°)				1.325	1.066
Ramachandran plot					
Favored (%)				98.8	98.8
Allowed (%)				1.2	1.2
Disallowed (%)				0	0

* The number in parenthesis is the shell at conventional cut off using I/σI=2 as criteria.

† 5% of reflections were used for calculation of $R_{free.}$

Supplementary Figure Legends

Fig. S1. Biochemical properties and disulfide bond linkage of con-ikot-ikot toxin. (**A**) Non-reducing SDS-PAGE gel of purified recombinant toxin. (**B**) Elution profile of purified recombinant toxin on a Superdex 75 size exclusion chromatography column is shown in red. The elution peaks of standards with molecular masses of 29.0 kDa and 12.4kDa are shown in grey. The molecular weight of recombinant toxin monomer is 9.7 kDa. (**C**) Disulfide linkage of a pattern of con-ikot-ikot toxin. The helices of toxin are shown in magenta. Cysteine positions are labeled as "C" in yellow. The linkages between cysteine resides, as determined by the crystal structure, are indicated by yellow lines. There are 10 intermolecular disulfide bonds and 3 intra-molecular bonds for a total of 13 disulfide bonds.

Fig. S2. Action of con-ikot-ikot toxin on GluA2 receptors. (**A,B,C,D,E**) Whole cell patch clamp recording of the GluA2 receptor. Black bars above the trace show application of 10mM glutamate. Black arrows show incubation of the clamped cell with toxin for 5-10 min. Recordings on wild type GluA2 are shown in panels A and C. Recordings on $GluA2_{cryst1}$ are shown in panels B and D. Recordings on $GluA2_{cryst2}$ are shown in panels E. Arrows in panel A and B denote incubation of crude *Conus Striatus* venom. Arrows in panel C,D and E denote incubation with 500 nM of recombinant venom. (**F**) Scintillation proximity assay (SPA) binding experiments measuring the ^{3}H FW binding to the $GluA2_{cryst1}$ construct in the presence of (R,R)-2b, toxin, and (R,R)-2b and toxin. Data are fitted by single site binding model. Shown are the mean values ± standard error of the mean based on in three replicates. Because we obtain crystals in the same crystal form without modulator and because toxin alone potently blocks desensitization, we propose that the toxin alone stabilizes the D1 – D1 interface in an intact conformation as in toxin-modulator complex observed here, as they share the same mechanism to prevent desensitization but bind to the receptor at different sites.

Fig. S3. GluA2-toxin interactions and LBD clamshell closure. (**A**) Sequence alignment of selected iGluRs amino acid sequences at the key sites for toxin interaction. Conserved residues are shown in red.

(**B**) Structure comparison of the KA+toxin+(R,R)-2b structure (shown in gray) and the FW+toxin+(R,R)-2b structure (LBD shown in blue and toxin shown in purple). Only the E subunit of the toxin and the LBD from the A subunit of GluA2 are shown. The toxin E subunit is used in structural alignment. The Cα atoms of K458 are used as marker atoms and are shown as spheres. The Cα of K458 of the apo sLBD following super imposition of the D2 lobe is shown as orange sphere. (**C**) Close-up view of the GluA2-toxin interaction sites. Key interactions between toxin E48 and GluA2 R660 and between toxin Q37 and GluA2 R453 are shown. Notably, there are 3.2 Å and 7.0 Å shifts of the Cα atoms of K458 between KA and FW and between KA and apo structures, respectively, due to different degrees of clamshell closure. (**D**) Reducing SDS-PAGE analysis of the SEC peak of the GluA2-toxin complex. Sample (a) is full length GluA2 protein mixed with crude *Conus striatus* venom, in the presence of FW. Sample (b) is GluA2 protein mixed with purified recombinant toxin, in the presence of FW. Sample (c) is the same as Sample (b) except without FW. Reduced toxin monomer position is labeled by an asterisk. (**E).** The soluble LBD structure with KA bound (PDB code 1FW0), showing the two distances ξ1 and ξ2 used to describe domain closure. ξ1 is the distance between the centers of mass (COMs) of residues 479–481 and residues 654–655. ξ_2 is the distance between the COMs of residues 401–403 and residues 686–687. Distances are plotted in panel (**F**).

Fig. S4. **I633 coupling switch mutants**. (**A,D,G,J,M**) Whole cell patch clamp recordings of wild type GluA2 (A), the I633A mutant (D), the I633E mutant (G) and the I633A mutant coexpressed with TARP γ2 (M). The black bar above the traces denotes application of 10 mM glutamate. The gray bar above the traces denotes continuous application of 300 μM cyclothiazide (CTZ). Statics of steady state currents recorded from wild type GluA2, I633A and I633E mutants are shown in (J) data is presented as ±SEM, n=5. (**B,E,H**) Fluorescence-detection size-exclusion chromatography (FSEC) profiles of wild-type GluA2 (B), the I633A mutant (E) and the I633E mutant (H). (**C,F,I,K,L**) FACS analysis of cell surface expression of wild-type GluA2 (C), I633A (F) and I633E (I). Negative control of untransfected cell with both primary and secondary antibodies is shown in panel K. A negative control experiment using cells

transfected with GFP-tagged wild-type GluA2 and secondary antibodies is shown in L. (**N**) Sequence alignment of selected iGluR sequences near the I633 coupling switch site. Residue I633 or its equivalent is in red.

Fig. S5. Electron density maps. (**A**) A 2mFo-DFc electron density map of the toxin in $GluA2_{cryst1}$, FW+(R,R)-2b+toxin structure. The map is contoured at 1.5σ. (**B-F**) A 2mFo-DFc map of the D2-M3 linker and M3 of chain B and D. Electron density map of the $GluA2_{cryst1}$, FW+(R,R)-2b+toxin structure is shown in panel B and the map is contoured at 0.9σ. An electron density map of the $GluA2_{cryst1}$, KA+(R,R)-2b+toxin structure is shown in panel C and the map is contoured at 0.9σ. An electron density map of $GluA2_{cryst2}$, KA+(R,R)-2b+toxin is shown in panel D and the map is contoured at 0.9σ. An electron density map of GluA2.A622T, KA+(R,R)-2b+toxin is shown in panel E and the map is contoured at 0.8σ. An electron density map of GluA2.T625G, KA+(R,R)-2b+toxin is shown in panel F and the map is contoured at 0.8σ. (**G**) A phased anomalous difference electron density map of Hg-labeled S635C at LBD-TM linker region. The map is contoured at 3.0σ.

Fig. S6. Stereo figures of structure comparison between GluA2 KA+toxin+(R,R)-2b and A622T GluA2 mutant KA+toxin+(R,R)-2b complex. The main chain atoms of the site of mutation, A622, are illustrated in orange. (**A**) Cα trace of the LBD D2 to M3 connections in the B/D subunits. The structure of the GluA2 KA+toxin+(R,R)-2b elements are shown in gray and those derived from the A622T GluA2 mutant KA+toxin+(R,R)-2b complex are shown in green. (**B**) The LBD D2 to M3 connections in A/C subunits. The structure of the GluA2 KA+toxin+(R,R)-2b complex is shown in gray and the structure of the A622T GluA2 KA+toxin+(R,R)-2b complex is shown in blue. (**C**) The close-up view of M3 tip and I633 binding site of B/D subunit. The structure of the GluA2 KA+toxin+(R,R)-2b elements (I633-uncoupled structure) are shown in gray and those derived from the A622T GluA2 mutant KA+toxin+(R,R)-2b complex (I633-coupled structure) are shown in green. Distances between Cα of V626 from intact M3 tip and Cαs of S631 from both structures are shown by dash. Chemical structure of positive modulator (R,R)-2b (**D**), FW (**E**) and KA (**F**).

Supplementary Movie Legends

Suppl. Movie M1: Morph illustrating the transition from an antagonist-bound GluA2 receptor conformation to a toxin + partial agonist FW + modulator (R,R)-2b-bound GluA2 conformation. This movie illustrates the symmetrical binding of the toxin dimer (magenta cartoon representation) between ATD and LBD layers of the GluA2 receptor, involving both intra- and inter-dimer interactions with the D1 lobes of all four chains, and with D1 and D2 lobes of the AC pair. Apart from toxin binding, the movie also highlights some key structural changes in the LBD region upon activation of the receptor by the partial agonist FW, including domain closure and the concomitant separation of the D2 lobes. The movie cycles several times between the previously published structure in complex with antagonist ZK200775 (ZK) and a toxin/receptor complex structure with partial agonist FW and the positive allosteric modulator (R,R)-2b. The respective current state in the movie (ZK or FW+(R,R)-2b)+toxin) is indicated by the label in the left lower corner. Ligand and modulator (R,R)-2b molecules are shown as grey or orange spheres, respectively. Receptor chains are colored the same as in previous figures (chains A and C in blue, chains B and D in green). The ATD layer of the receptor is only shown once for the ZK-bound structure at the beginning of the movie and omitted in the rest of the movie.

Suppl. Movie M2: Morph illustrating the transition from an antagonist-bound GluA2 receptor conformation to a toxin + partial agonist KA + modulator (R,R)-2b-bound GluA2 conformation. The movie shows the same transition and receptor views as Movie M1 except here the toxin binds to the receptor in presence of the partial agonist KA and modulator (R,R)-2b.

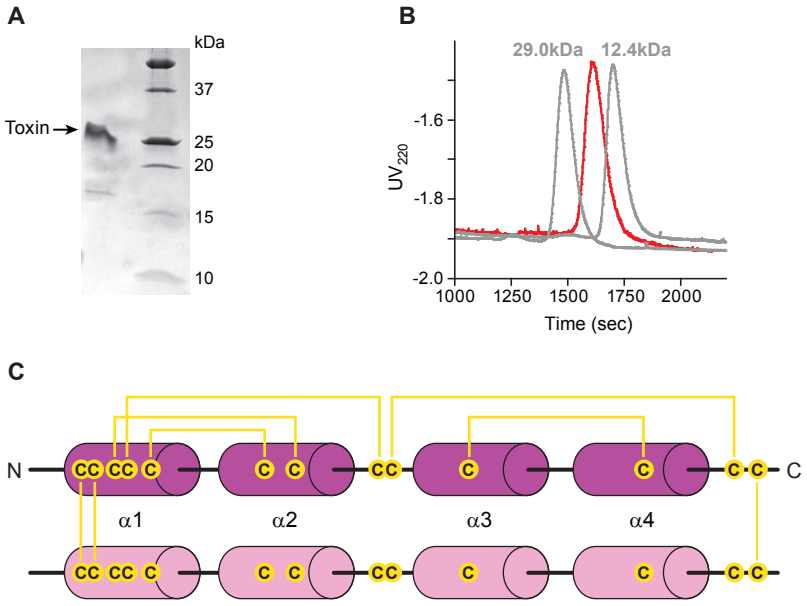

Chen Figure S1

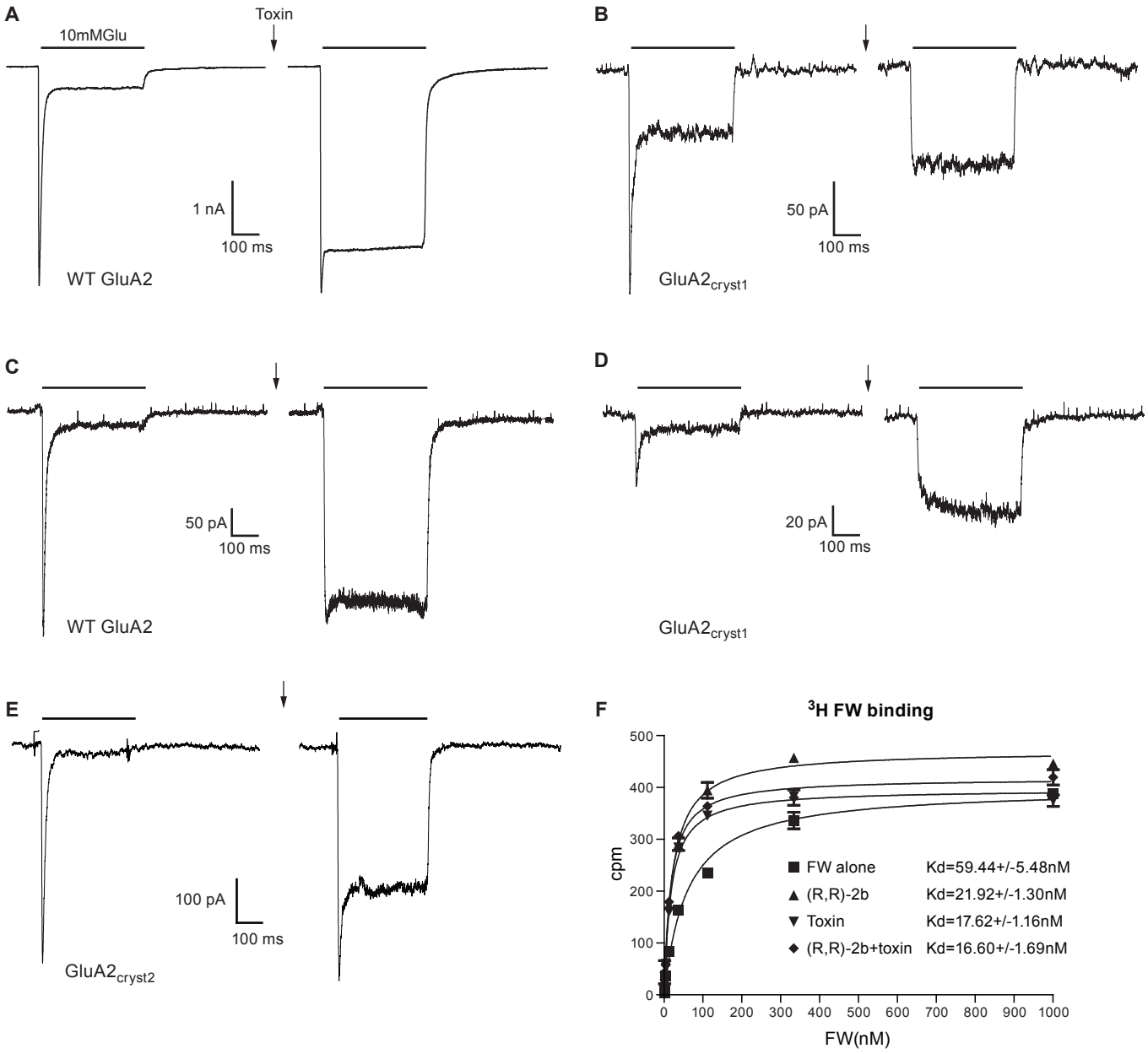

Chen Figure S2

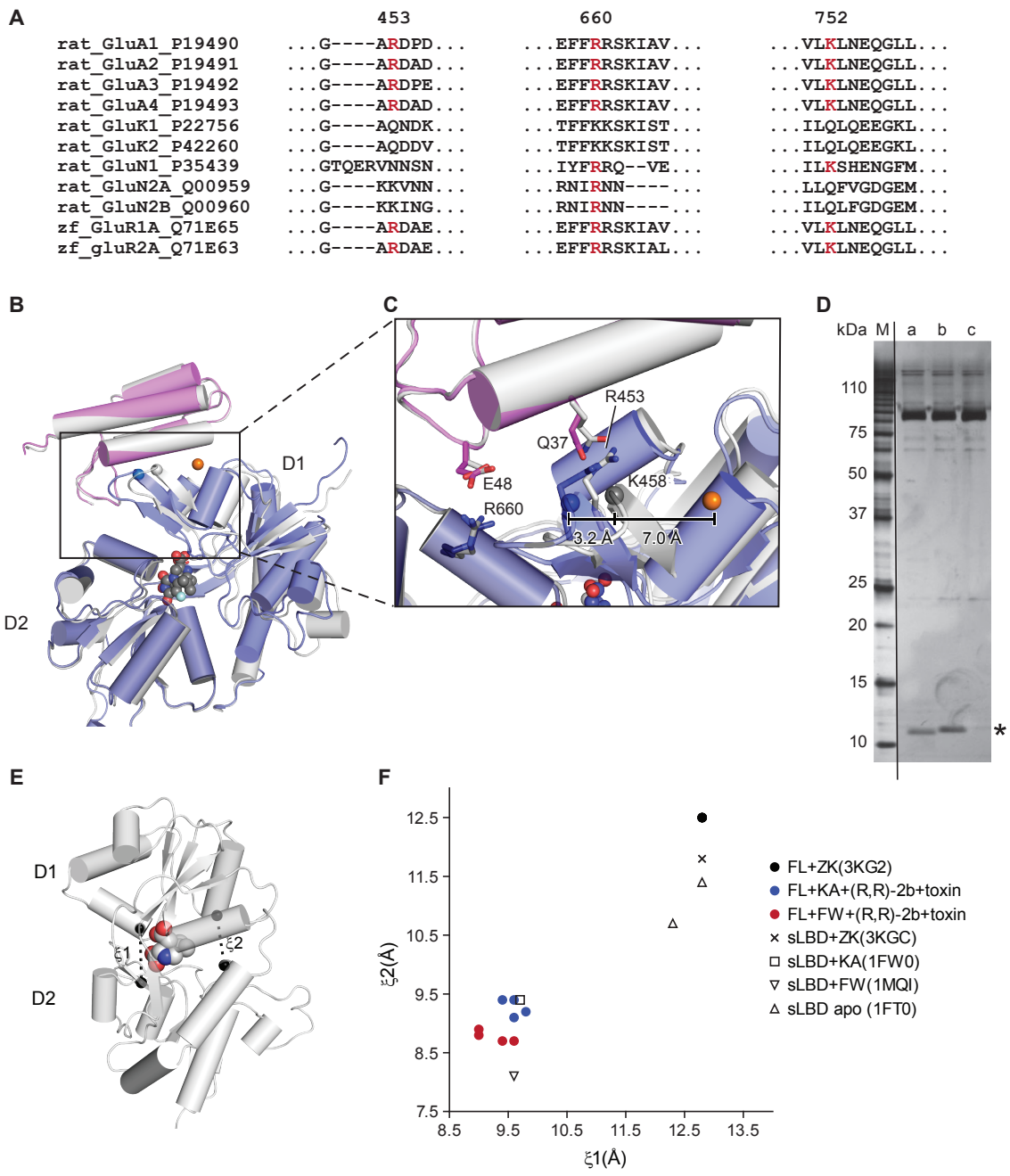

Chen Figure S3

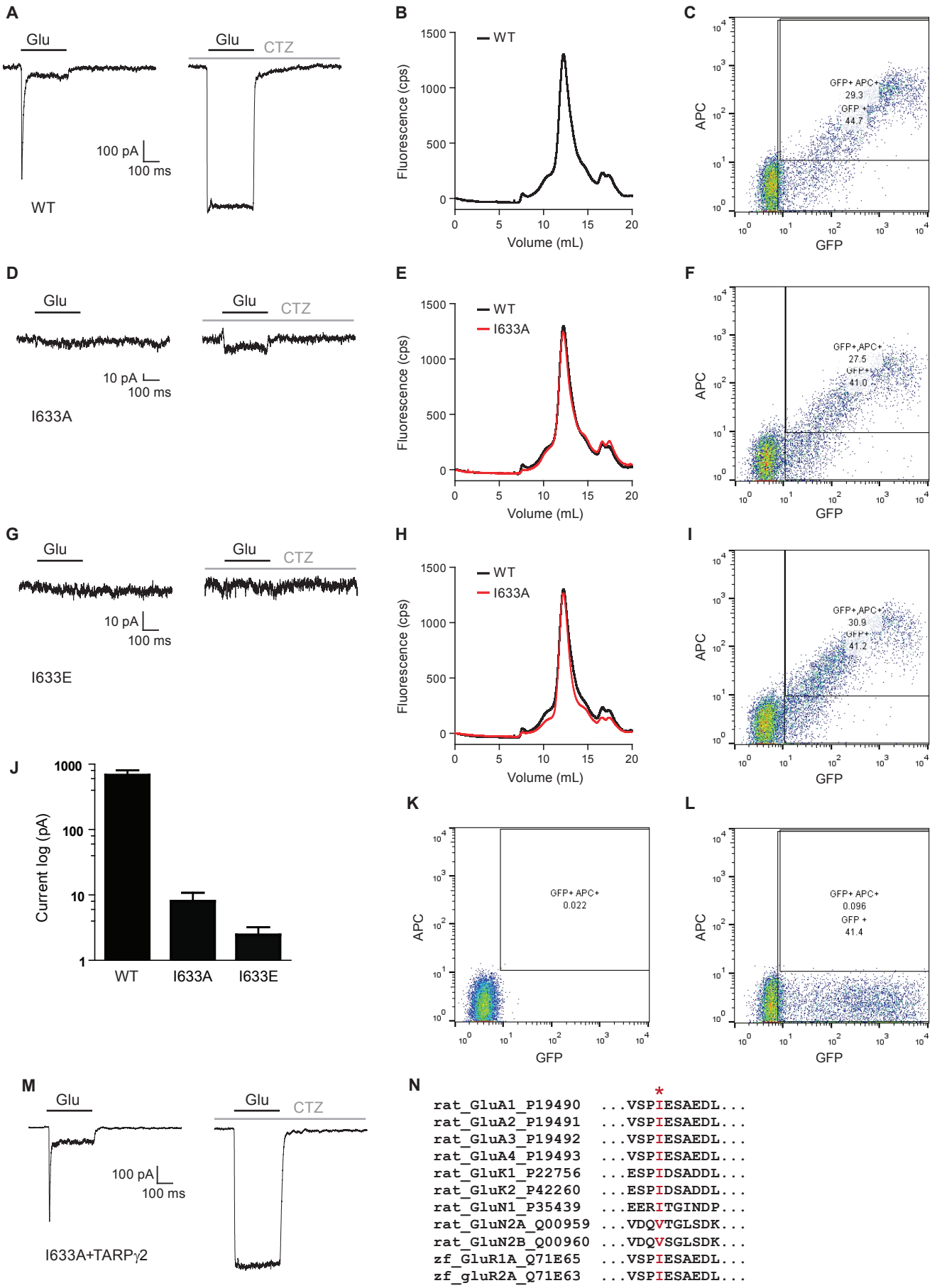

Chen Figure S4

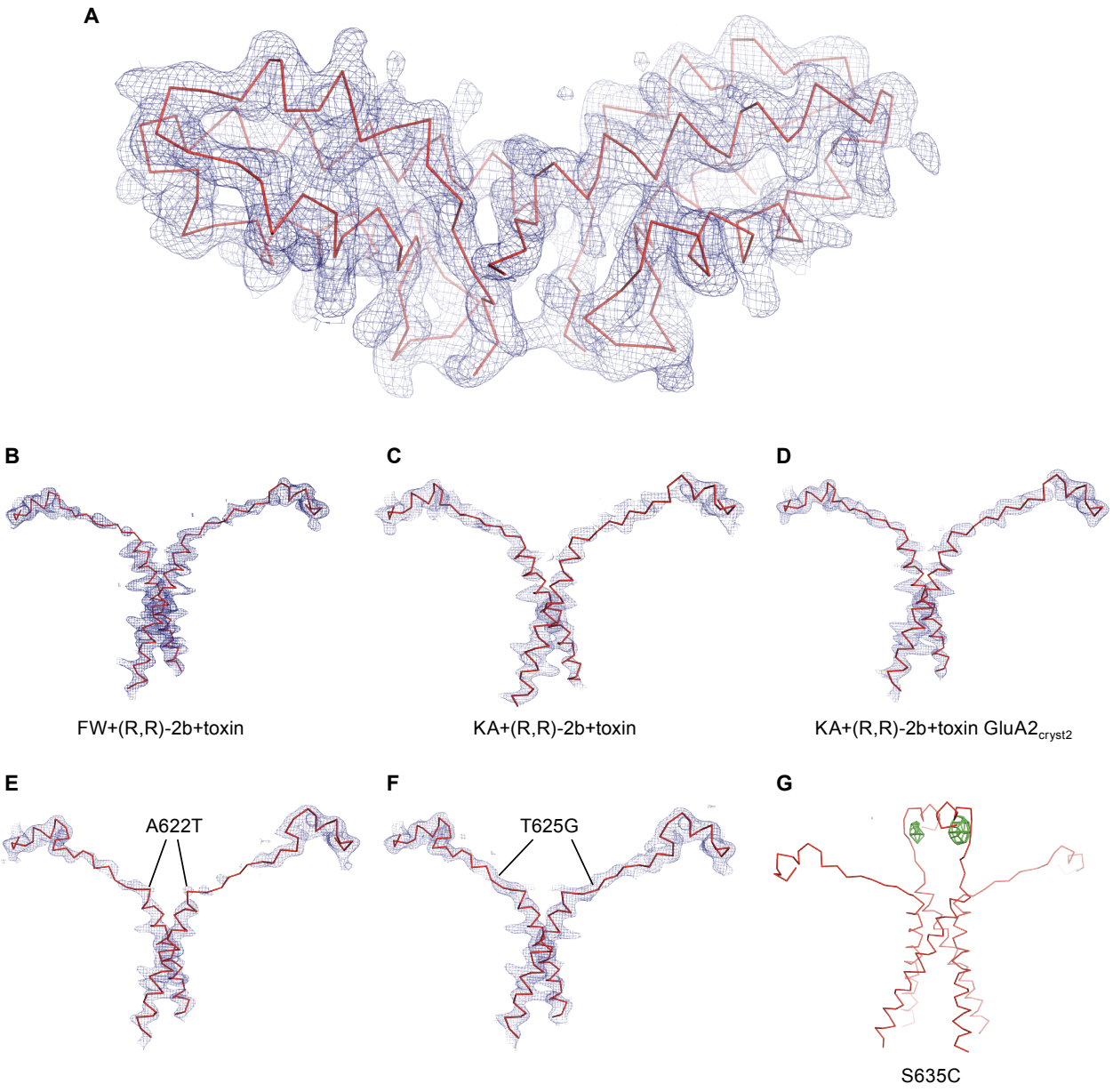

Chen Figure S5

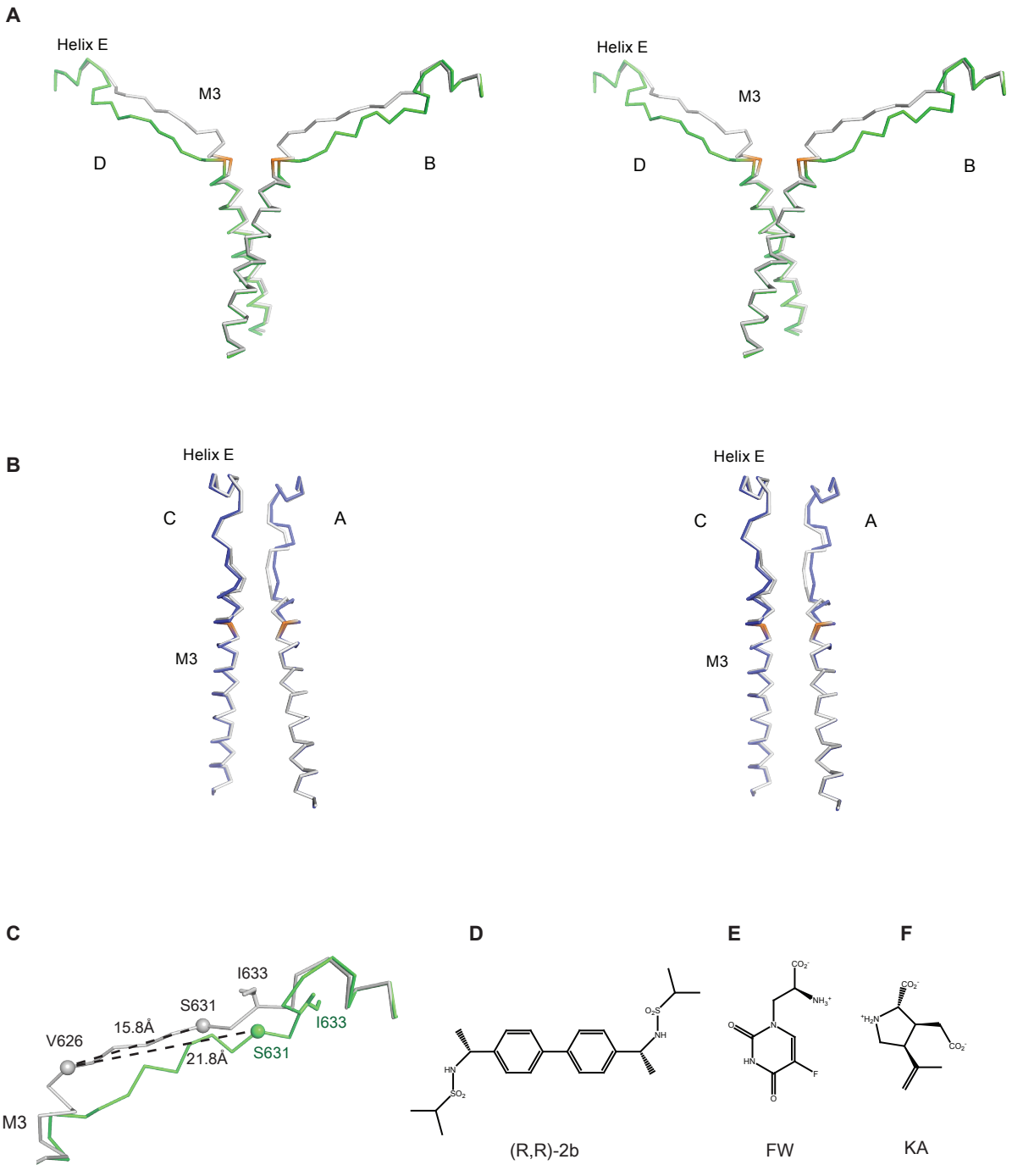

Chen Figure S6